

DEUTSCHES ELEKTRONEN-SYNCHROTRON

Ein Forschungszentrum der Helmholtz-Gemeinschaft

DESY 11-096

June 2011

**Circular polarization control for the European
XFEL in the soft X-ray regime**

Gianluca Geloni,
European XFEL GmbH, Hamburg

Vitali Kocharyan and Evgeni Saldin
Deutsches Elektronen-Synchrotron DESY, Hamburg

ISSN 0418-9833

NOTKESTRASSE 85 - 22607 HAMBURG

Circular polarization control for the European XFEL in the soft X-ray regime

Gianluca Geloni,^{a,1} Vitali Kocharyan^b and Evgeni Saldin^b

^a*European XFEL GmbH, Hamburg, Germany*

^b*Deutsches Elektronen-Synchrotron (DESY), Hamburg, Germany*

Abstract

The possibility of producing X-ray radiation with high degree of circular polarization is an important asset at XFEL facilities. Polarization control is most important in the soft X-ray region. However, the baseline of the European XFEL, including the soft X-ray SASE3 line, foresees planar undulators only, yielding linearly-polarized radiation. It is clear that the lowest-risk strategy for implementing polarization control at SASE3 involves adding an APPLE II - type undulator at the end of the planar undulator, in order to exploit the micro bunching from the baseline FEL. Detailed experience is available in synchrotron radiation laboratories concerning the manufacturing of 5 m - long APPLE II undulators. However, the choice of a short helical radiator leads to the problem of background suppression. The driving idea of our proposal is that the background radiation can be suppressed by spatial filtering. This operation can be performed by inserting slits behind the APPLE II radiator, where the linearly-polarized radiation spot size is about 30 times larger than the radiation spot size from the helical radiator. The last 7 cells of the SASE3 undulator are left with an open gap in order to provide a total 42 m drift section for electron beam and radiation. Due to the presence of the drift the linearly-polarized radiation spot size increases, and the linearly polarized background radiation can be suppressed by the slits. At the same time, the microbunch structure is easily preserved, so that intense (100 GW) coherent radiation is emitted in the helical radiator. We propose a filtering setup consisting of a pair of water cooled slits for X-ray beam filtering and of a 5 m-long magnetic chicane, which creates an offset for slit installation immediately behind the helical radiator. Electrons and X-rays are separated before the slits by the magnetic chicane, so that the electron beam can pass by the filtering setup without perturbations. Based on start-to-end simulations we present complete calculations from the SASE3 undulator entrance up to the radiator exit including the modulated electron beam transport by the FODO focusing system in the low charge (20 pC) mode of operation.

¹ Corresponding Author. E-mail address: gianluca.geloni@xfel.eu

1 Introduction

The European XFEL [1], which is currently under construction, will be equipped with planar undulators providing linearly polarized radiation in the horizontal plane. While it will be possible to change the photon energy by opening or closing the gap of the undulators at different operation energies, polarization control remains problematic. However, circularly polarized X-ray radiation is an important tool for investigating magnetic materials and other material science issues, especially in the soft X-ray region. In particular, the spectral range between 550 eV and 900 eV covers absorption edges of transition metals which are of relevance for technological applications: Cr, Mn, Fe, Co, and Ni. This spectral region can be covered by the SASE3 undulator in the fundamental harmonic at the nominal electron beam energy of 14 GeV.

The possibility of generating variably polarized radiation at SASE3 was recently investigated at the European XFEL and DESY. Several optimized schemes were considered [2]-[6]. All these schemes exploit the microbunching generated in the planar undulator, and make use of a short helical radiator at the end of the SASE3 undulator. However, the exploitation of the microbunching from the planar undulator leads to background problems, since the linearly-polarized radiation from the planar undulator should be suppressed.

In order to solve the background issue it has been proposed [6] that the radiation in the helical radiator can be tuned to the second harmonic and be therefore characterized by a different frequency compared to the linearly polarized radiation. However, for the European XFEL this option cannot cover the most interesting region between 550 eV and 900 eV at the nominal electron beam energy of 14 GeV. It will cover this wavelength range only at 10 GeV, but in this case the hard X-ray lines SASE1 and SASE2 will not be able to operate at Angstrom wavelength range. Another drawback of using second harmonic helical radiators is that in order to achieve a spectral separation of radiation at the first and at the second harmonic, an extra dispersive X-ray optics element needs to be introduced in the photon beam line. Such type of element has not yet come into operation.

Another possible solution to the background problem has been proposed in [2]-[5]. In this option, the electron beam is deflected by a bending system after the planar undulator and subsequently passes through the helical radiator. In this way the linearly polarized radiation is separated from the circularly polarized one, and the polarization properties of the radiator are completely decoupled from those of the light produced in the planar undulator. However, the electron beam microbunching must be preserved

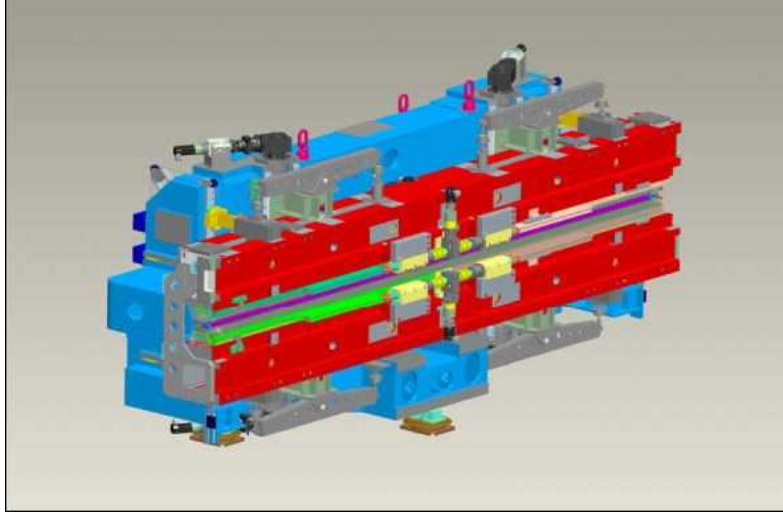


Fig. 1. Mechanical layout of an APPLE II undulator module (Courtesy of M. Tischer).

through the bending system on the scale of the soft X-ray radiation wavelength produced in the planar undulator, and this constitutes a challenge, which began to be addressed in literature only very recently [5].

In this paper we propose a third option, which makes use of an in-line setup. After the passage through the planar undulator, the electron beam is sent through a straight section drift, and subsequently through a short APPLE II radiator tuned at the fundamental harmonic. The background radiation from the planar undulator is suppressed by a spatial filtering setup consisting of a water cooled slits pair for X-ray beam filtering and of a 5 m-long magnetic chicane, which creates an offset for slit installation immediately behind the helical radiator. Electrons and X-rays are separated before the slits by the magnetic chicane, so that the electron beam can pass by the filtering setup without perturbations. Compared to the method proposed in [7] for the LCLS, the introduction of the chicane allows to ease the requirements on the thin Berillium slits in [7], and allows for the installation of water-cooled power slits of any material to cope with the increased heat loading due to the high repetition rate of the European XFEL. However, it should be noted that the method is applicable at other facilities, including as well the LCLS. The helical radiator is placed immediately behind the SASE3 undulator, consisting of 21 cells. The last 7 cells of the SASE3 undulator are left with an open gap in order to provide a total 42 m drift section for electron beam and radiation. Due to the presence of the drift, the linearly-polarized radiation spot size at the slits is about 30 times larger than the circularly-polarized one, and the linearly polarized background can be easily suppressed by the slits. At the same time, the in-line design allows to preserve the microbunching structure. Intense coherent radiation in the 100 GW level is emitted in the helical radiator.

Microbunch preserving in-line scheme for helical radiator
with spatial filtering out the linearly-polarized radiation

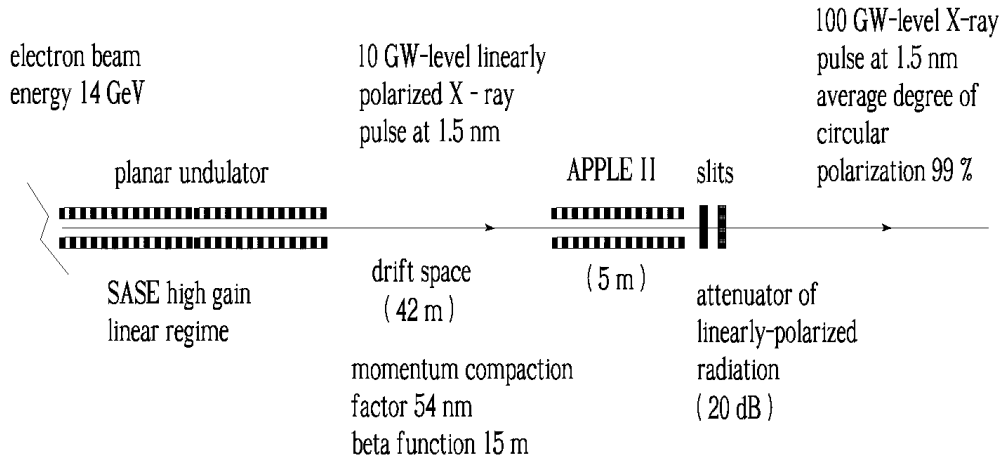


Fig. 2. Concept for circular polarization control at the European XFEL. After the planar SASE3 undulator line, the electron beam is propagated along a 42 m-long (7 cells of SASE3) straight section. Subsequently, it passes through a helical radiator. The microbunch is preserved, and intense coherent radiation is emitted in the helical radiator. Linearly-polarized radiation from the planar undulator is easily suppressed by spatial filtering with the help of slits downstream of the helical radiator, which do not attenuate the circularly-polarized radiation from the helical radiator. The electron beam flies by the slit system following a magnetic chicane, see Fig. 4.

Simulations performed with the code GENESIS show that in order to transport the microbunched electron beam through the 42 m-long straight section (corresponding to the 7 undulator modules with open gap), it is sufficient to use the existing undulator FODO structure with the usual (15 m) beta function as a focusing system. The proposed option has advantages in terms of cost and time, also because we can afford to use the existing design of APPLE II type undulators, Fig. 1, improved for PETRA III [8].

2 Scheme for circular polarization control based on spatial filtering of the linearly-polarized radiation background behind the helical radiator

The principle of our scheme for polarization control at the European XFEL is illustrated in Fig. 2, Fig. 3, Fig. 4 and Fig. 5.

With reference to Fig. 2, the electron beam first goes through the SASE3 baseline undulator, it produces linearly polarized SASE radiation, and is

installation of the helical radiator downstream of the SASE 3 undulator

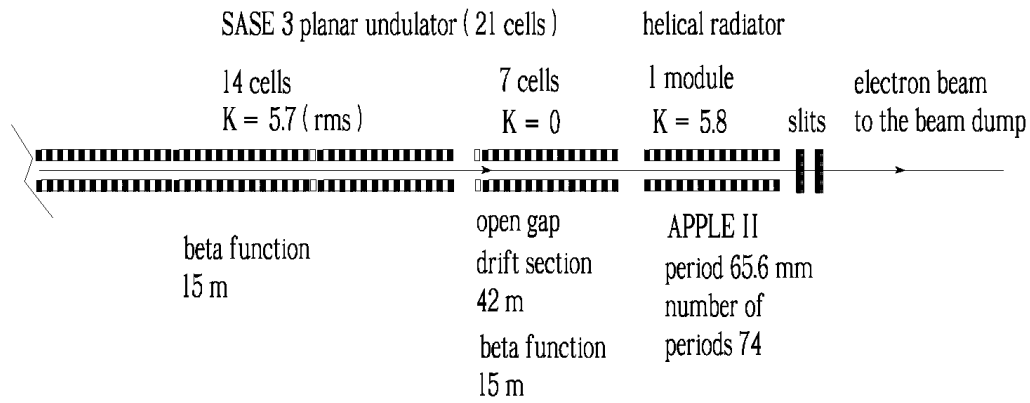


Fig. 3. The installation of helical radiator and spatial filtering setup downstream of the SASE3 undulator will allow to produce high-power, highly circularly-polarized soft X-ray radiation.

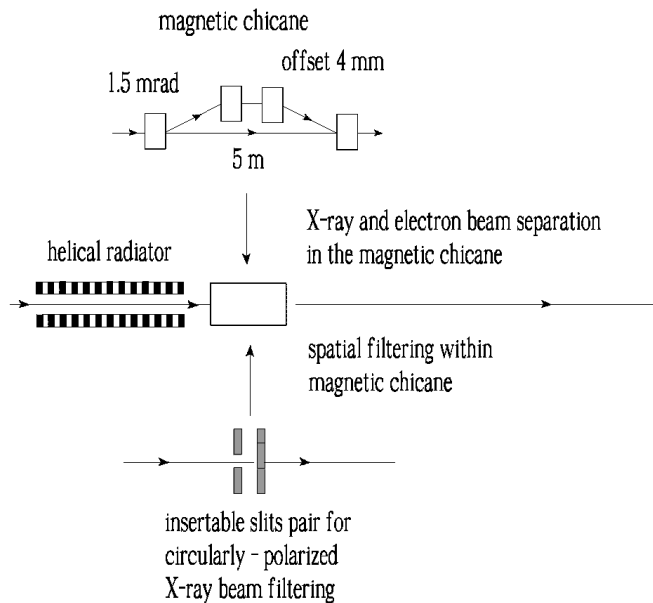


Fig. 4. The scheme for spatial filtering will make use of a short magnetic chicane immediately behind the helical radiator, so that the electron beam can bypass the slits.

modulated both in energy and density. The last seven SASE3 undulator modules are left with the gap open, Fig. 3. In this way we provide a total 42 m - long straight section for radiation and electron beam transport, corresponding to the length of the 7 undulator cells. At the end of the straight section, that is immediately behind the entire (21 cells) SASE3 undulator,

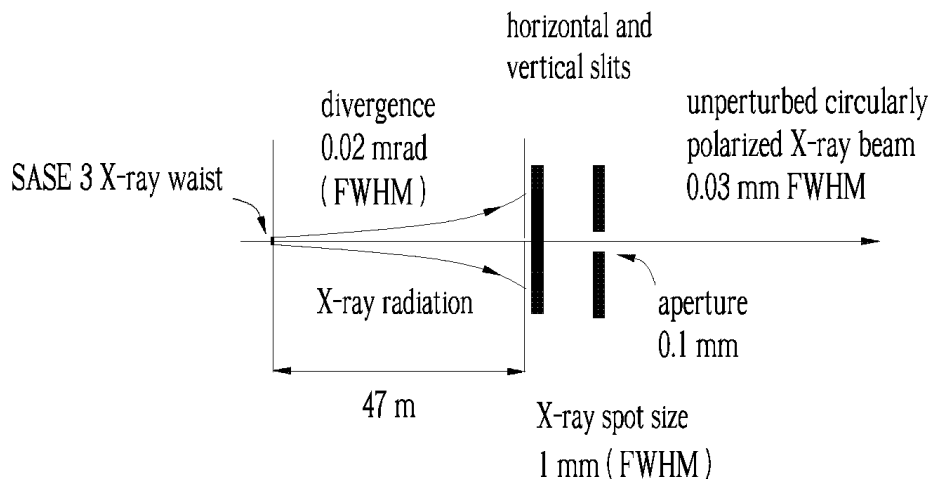


Fig. 5. Simple method for suppressing the linearly-polarized soft X-ray radiation from the SASE3 undulator. The linearly-polarized background can be eliminated by using a special window positioned downstream of the helical radiator exit. This can be practically implemented by letting radiation and electron beam through vertical and horizontal slits positioned 47 m downstream the planar undulator, where the linearly-polarized radiation pulse is characterized by a spot size thirty times larger than that of the circularly-polarized radiation pulse.

we install a 5 m - long APPLE II type undulator module. While passing through this helical radiator, the microbunched electron beam produces intense bursts of radiation in any selected state of polarization. Subsequently, the circularly polarized radiation from the APPLE II undulator, the linearly-polarized radiation from the SASE3 undulator and the electron beam pass through a spatial filtering station.

A schematic of the spatial filtering station is shown in Fig. 4. It consists of a magnetic chicane, which allows for the electron beam to pass by an insertable pair of slits, which is the main part of the filtering station. Since the slits are positioned 47 m downstream of the planar undulator, the linearly-polarized radiation is characterized by a 0.9 mm FWHM spot size, which is about 30 times larger compared to the circularly-polarized radiation spot size, amounting to about 0.03 mm FWHM. At the slit aperture of 0.1 mm the background radiation power can therefore be diminished of two orders of magnitude without perturbing the circularly polarized radiation pulse, Fig. 5. The short chicane allows to decouple the electron beam trajectory from the radiation. This is required at the European XFEL, in order to leave complete freedom for the slit design. In fact, if the electron beam passes through the slits, ionization losses must be kept to a negligible level, and this poses constraints on the slit thickness and material. For example, for the

Table 1

Parameters for the low-charge mode of operation at the SASE3 line of the European XFEL used in this paper.

	Units	
Undulator period	mm	68
N periods/module	-	74
Intersection length	cm	108
K parameter (rms)	-	5.7
Wavelength	nm	1.5
Energy	GeV	14
Charge	nC	0.02
Average beta function	m	15

LCLS we previously proposed to use 150 μm -thick Berillium slits [7]. Due to the very high repetition rate and burst structure of the European XFEL output, such solution is not optimal. With the use of the chicane instead, the issues of electron beam transport to the dump and of that of background radiation filtering are fully decoupled, so that the slit design can fulfill the most stringent engineering constraints to cope with heat-loading issues. This idea can straightforwardly be implemented, when needed, at other facilities as well.

The influence of the propagation of the electron beam through the drift section on the electron beam microbunching should be accounted for. In particular, one should account for the fact that the straight section acts as a dispersive element with momentum compaction factor $R_{56} \sim 60$ nm at the electron beam energy 14 GeV. The influence of betatron motion should be further considered. In fact, the finite angular divergence of the electron beam, which is linked with betatron function, leads to longitudinal velocity spread yielding microbunching suppression. In the next Section we will present a comprehensive study of these effects. We simulated the evolution of the microbunching along the straight section, and we concluded that the transport of the microbunched electron beam through the 42 m-long straight section does not constitute a serious problem for the realization of the proposed scheme.

3 FEL simulations

In this Section we report on a feasibility study performed with the help of the FEL code GENESIS 1.3 [9] running on a parallel machine. We will present

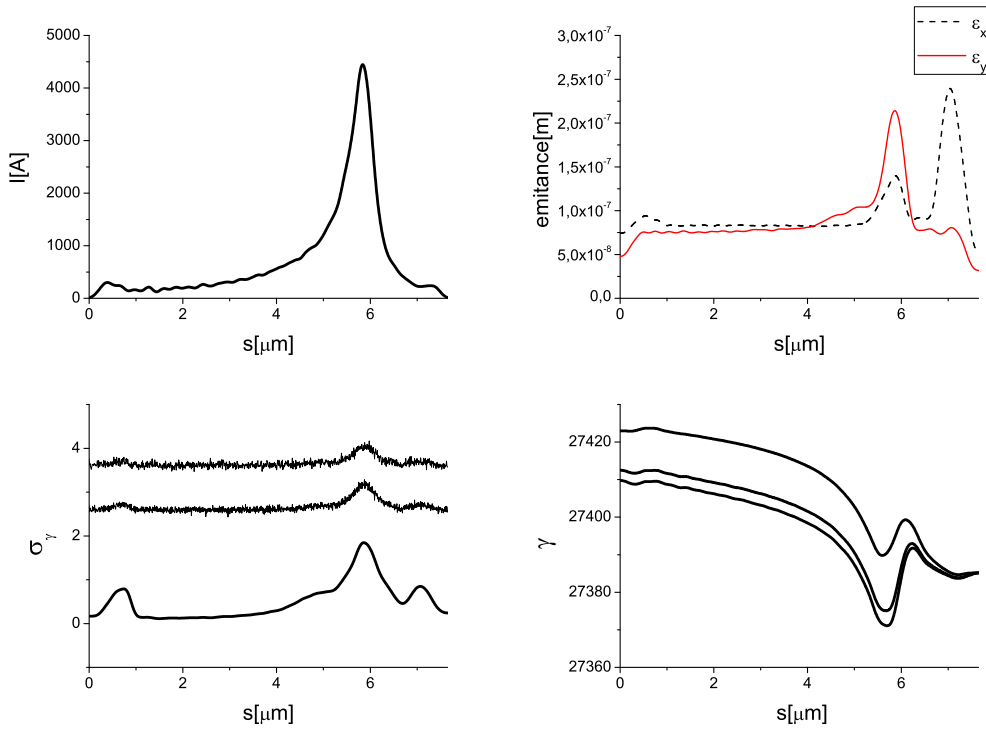


Fig. 6. The current profile (top left), and the horizontal and vertical emittances (top right) at the entrance of the SASE1 beamline. Energy spread (bottom left) and energy (bottom right) of the electrons at different positions down the beamline: at the entrance of the SASE1 undulator (lower curve), after SASE1 (middle curve) and at the entrance of the five working cells of SASE3 (upper curve).

a feasibility study for our method of polarization control at the European XFEL, based on a statistical analysis consisting of 100 runs. Parameters used in the simulations for the low-charge mode of operation (0.02 nC) are presented in Table 1. The choice of the low-charge mode of operation is motivated by simplicity. The input for GENESIS included start-to-end simulations of the electron beam characteristics. The top plots of Fig. 6 show the current profile and the emittances along horizontal and vertical directions at the entrance of SASE1 [10]. The bottom plots of the same Fig. 6 show the energy and the energy spread at three different locations: at the entrance of SASE1 following [10] (lower line), at the exit of SASE1 (middle line) and at the entrance of the 5 working cells of SASE3 (upper line). It should be noted here that the output of the device is optimized when the first 9 SASE3 modules are detuned from resonance. This means that only the last 5 SASE3 cells are working. The wake from the undulator vacuum chamber in Fig. 7, also obtained from [10], and quantum fluctuations are respectively responsible for the change in energy and energy spread of the electrons as in the bottom plots of Fig. 6.

First, the baseline SASE undulator output was simulated. The result, in terms of power and spectrum, is shown in Fig. 8, while the angular distribution of

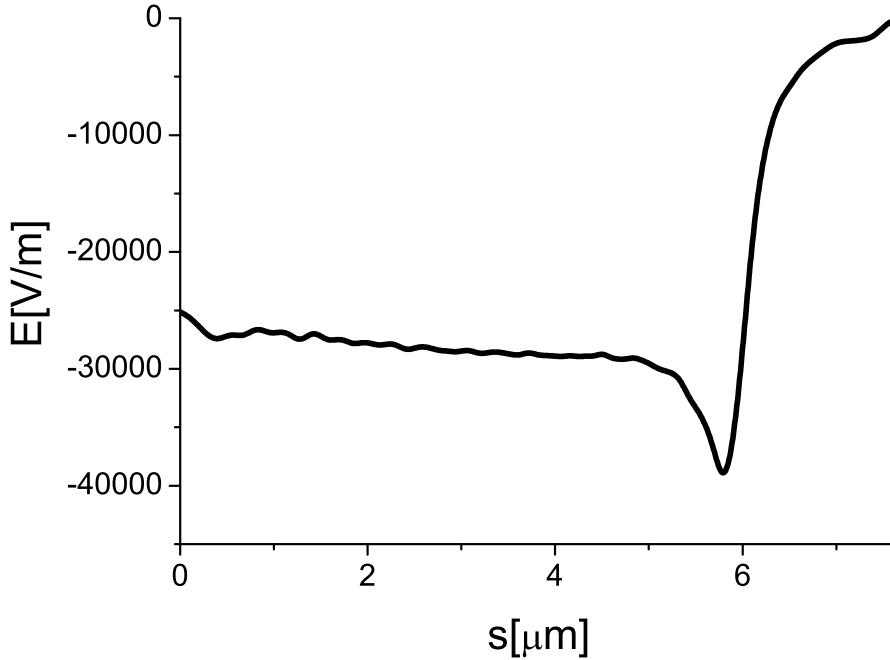


Fig. 7. The wakefield in SASE1 and in the first 9 cells of SASE3 (detuned).

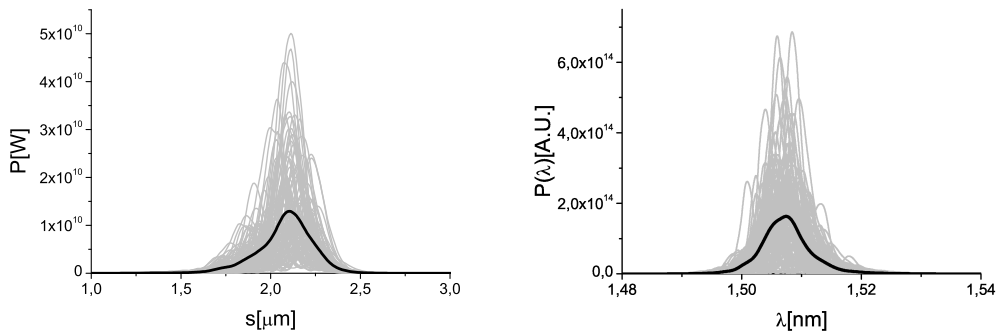


Fig. 8. Left plot: power distribution after the 5 active SASE3 undulator cells. Right plot: spectrum after the 5 active SASE3 undulator cells. Grey lines refer to single shot realizations, the black line refers to the average over a hundred realizations.

the radiation is shown in Fig. 9. In order to obtain Fig. 9, we first calculated the intensity distribution along the bunch, so that in the left plot we present the energy density as a function of the transverse coordinates x or y , as if it was measured by an integrating photodetector. Finally, a two-dimensional Fourier transform of each slice of the GENESIS field file was performed. These Fourier transformed data were squared and summed over the slice, yielding the angular X-ray radiation pulse energy distribution. The x and y cuts are shown on the right plot.

The GENESIS particle file was downloaded at the exit of the baseline un-

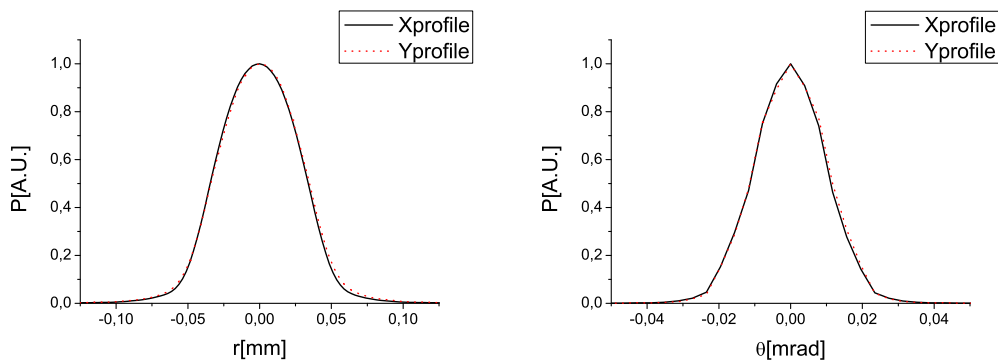


Fig. 9. Left plot: Transverse plot of the X-ray radiation pulse energy distribution after the SASE3 undulator (5 active cells). Right plot: Angular plot of the X-ray radiation pulse energy distribution after the SASE3 undulator (5 active cells).

ulator. For simulating the straight section in GENESIS we used the same 5-cells undulator structure as for the baseline undulator, but we changed the undulator parameter to $K = 0.01$. This choice allows one to have, with negligible differences, the same momentum compaction factor as in free space. Then the electron beam current was set to zero, and the undulator focusing was switched off (although for $K = 0.01$ the undulator focusing effects are negligible). The GENESIS particle file was used as an input for the propagation of the bunch along the 42 m-long FODO lattice. GENESIS automatically accounts for momentum compaction factor and betatron motion effects on the evolution of the microbunched beam. We tested the correctness of GENESIS simulations concerning the betatron motion effects in reference [11]. The bunching before and after the straight section drift is shown in Fig. 10, upper plot, as a function of the longitudinal coordinate inside the electron bunch, for a particular run. The evolution of the bunching at the position of the maximal peak current along the straight section for the same run is shown in Fig. 10, lower plot.

The evolution of the rms electron beam size in the horizontal and in the vertical direction inside the baseline undulator and in the straight section are shown respectively in Fig. 11. These plots correspond to the position with maximal peak current, and to normalized slice emittances $\varepsilon_x = 0.138 \mu\text{m}$ and $\varepsilon_y = 0.212 \mu\text{m}$. From the average rms beam size and the normalized emittances corresponding to the slice of maximal peak current we can conclude that the average betatron function used was about 15 m. Inspection of Fig. 11, right plot, shows a little mismatching in the vertical direction y , which is not present in the left plot. This is due to the fact that in baseline undulator the electron beam was matched accounting for the undulator focusing properties. However, the mismatch was accounted for, because we used the particle file at the exit of straight section as input file for GENESIS simulations of the APPLE II output, meaning that the particle file was downloaded again at the end of the propagation through the straight section. Note that

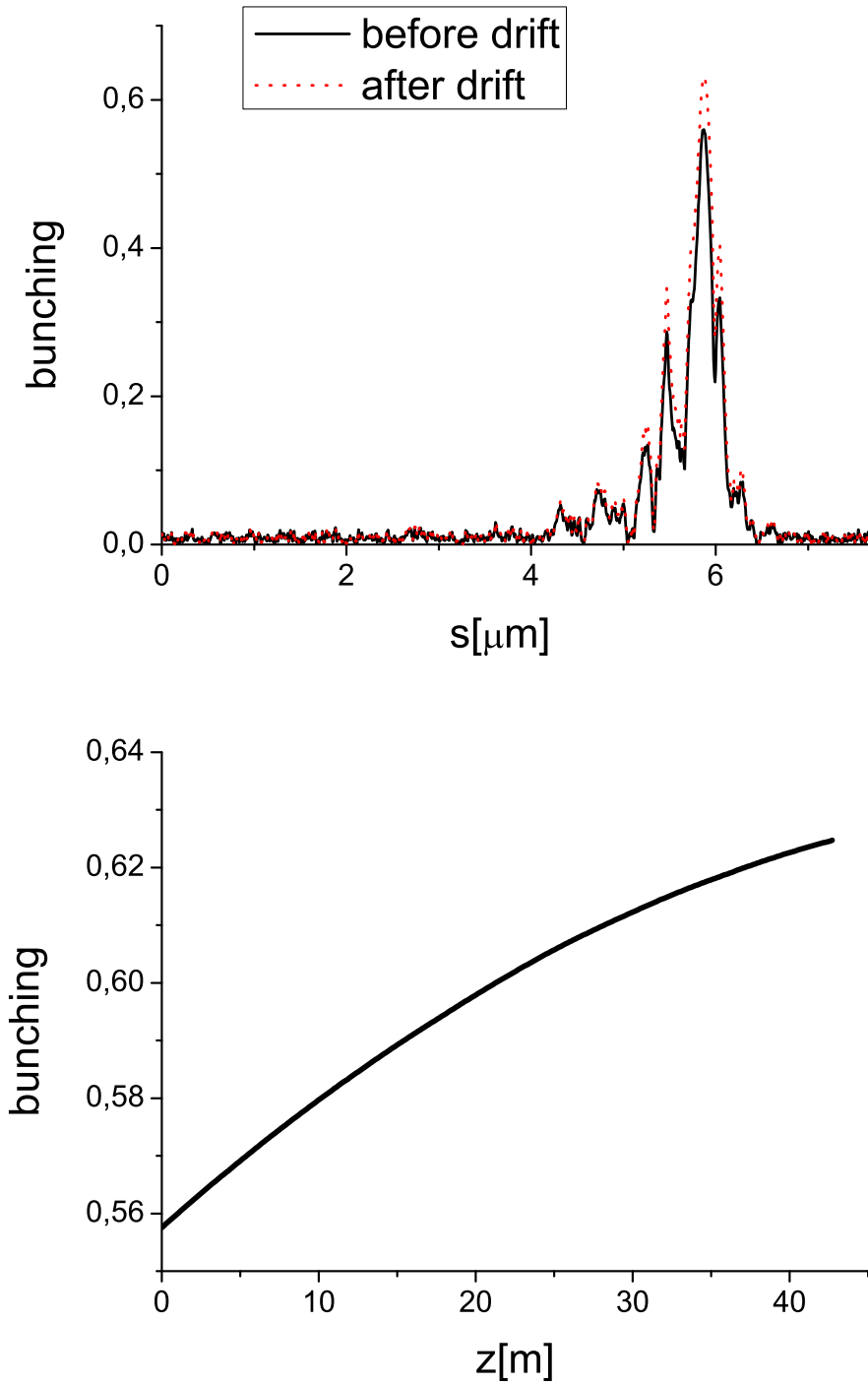


Fig. 10. Upper plot: comparison between the bunching before and after the drift for a particular FEL run. Lower plot: evolution of the bunching at the position of maximal current along the straight section for the same run.

each cell begins with an undulator, and finishes with a quadrupole. Therefore we downloaded the particle file immediately after the first quadrupole

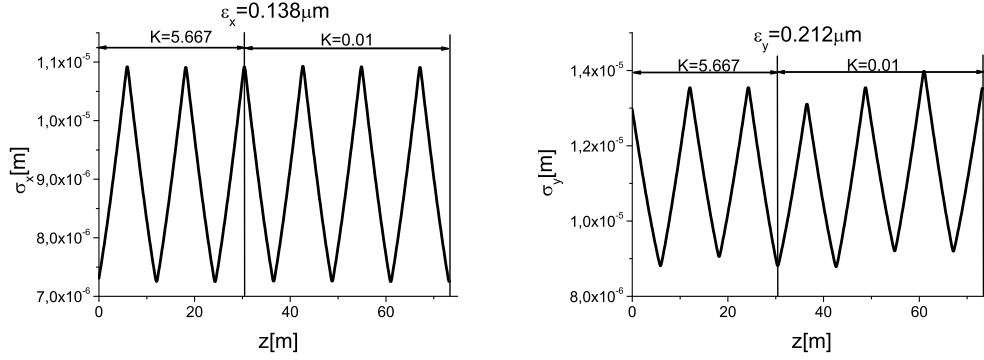


Fig. 11. Evolution of the rms horizontal (left plot) and vertical (right plot) beam size as a function of the distance along the setup calculated through GENESIS. The emittance reported is normalized, and corresponds to the position within the bunch where the current is maximal.

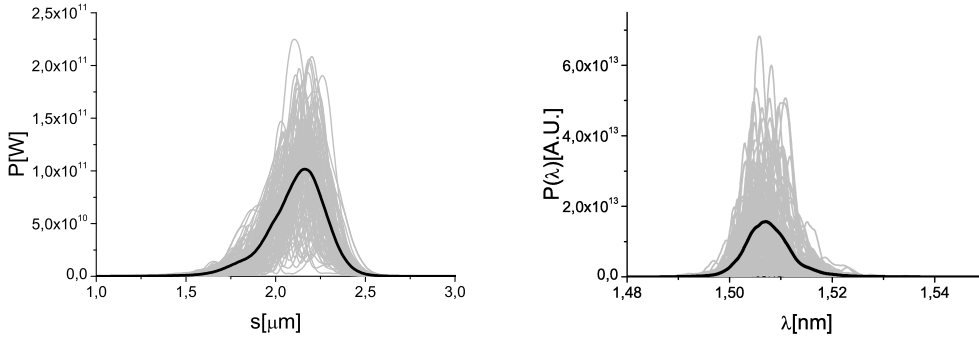


Fig. 12. Left plot: output power distribution from the APPLE II undulator. Right plot: output spectrum. Grey lines refer to single shot realizations, the black line refers to the average over a hundred realizations.

related with propagation inside the APPLE II undulator. The average betatron function is again $\beta = 15$ m. This guarantees correct propagation along the APPLE II undulator section, which is 5 m long. The output files are downloaded immediately after the APPLE II undulator.

The final output from our setup is shown in Fig. 12, left plot, in terms of power and in Fig. 12, right plot, in terms of spectrum. An output power in the order of 100 GW is granted, which is much larger than the SASE level reported in Fig. 8, and is about the same as the SASE power level at saturation, which we plot in Fig. 13 for comparison. One should appreciate the differences compared to the LCLS case [7], where the APPLE II output is of the same order of magnitude, but still a factor three smaller than the saturation level. First, in the SASE3 case we have a much smaller compaction factor ($R_{56} = 60$ nm compared to $R_{56} = 560$ nm at LCLS), a factor three smaller emittance, and a factor 1.5 larger beta function, while the drift space is only a factor two larger in the SASE3 setup. As a result, the parameter which controls the debunching induced by betatron oscillations, $[L\varepsilon/(\lambda\beta)]^2$

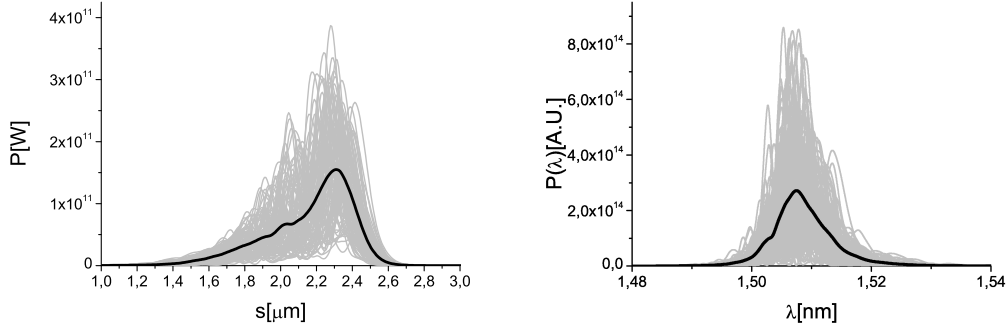


Fig. 13. Left plot: SASE3 power distribution at saturation (after 7 cells). Right plot: SASE3 spectrum at saturation (after 7 cells). Grey lines refer to single shot realizations, the black line refers to the average over a hundred realizations.

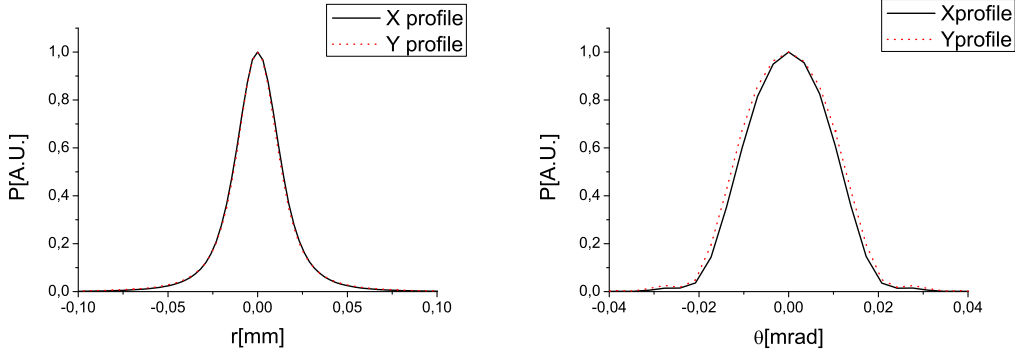


Fig. 14. Left plot: Transverse plot of the X-ray radiation pulse energy distribution after the APPLE II undulator (5 cells). Right plot: Angular plot of the X-ray radiation pulse energy distribution after after the APPLE II undulator (5 cells).

(see [11]) is a factor four smaller for the SASE3 setup, yielding a smaller effect. The modulation is almost frozen, and one can optimize the bunching at the APPLE II entrance to a level very near to the saturation point. Second, in SASE3 the period is very close to that of the APPLE II device, as they have practically the same K parameter ($K = 5.66$ rms for the SASE baseline compared to $K = 5.8$ for the APPLE II undulator). As a result, the APPLE II undulator effectively interacts with the electron beam. Since a helical undulator can be considered as a superposition, in the vertical an horizontal planes, of two planar cells, one can consider a 5 meter-long APPLE II cell equivalent to two planar cells, which help in the building up of extra-bunching, and in the overall output increase.

The transverse distribution of the radiation is shown in Fig. 14 in terms of transverse coordinates (left plot) and angles (right plot). From the analysis of Fig. 9 one finds an angular size in the order of $20 \mu\text{rad}$ FWHM. As a result, after 47 m propagation (including the drift an the APPLE II undulator), the transverse size of the SASE radiation is about 0.9 mm FWHM, to be

compared with the APPLE II radiation spot size, which is about $30 \mu\text{m}$. The SASE radiation spot size is, therefore, about 30 times larger than the APPLE II radiation spot size. Moreover, the ratio between circularly and linearly polarized peak power is about 10. A slit system letting through the FWHM of the APPLE II radiation would let pass a relative background radiation contribution (linearized polarized) of about $10^{-1} \cdot (30/900)^2 \sim 10^{-4}$, which is practically negligible.

4 Conclusions

The European XFEL does not offer the possibility of polarization control: the output radiation is simply linearly polarized. However, the production of light with variable polarization, and in particular of circularly polarized radiation is of most interest for many experiments, prevalently in the soft X-ray region. In this paper we demonstrated that such polarization control can be achieved with the help of an almost trivial setup, composed by three components: an APPLE II type undulator module, which is meant to be installed immediately behind the SASE3 undulator line, a short magnetic chicane, to be installed immediately behind the APPLE II undulator module, and an insertable slits pair, which is installed in the transverse offset created by the magnetic chicane, and serves for X-ray spatial filtering. The setup can be straightforwardly installed behind the SASE3 undulator and is safe, in the sense that it guarantees the baseline mode of operation. The proposed polarization control setup takes almost no cost and time to be implemented at the European XFEL.

5 Acknowledgements

We are grateful to Massimo Altarelli, Reinhard Brinkmann, Serguei Molodtsov and Edgar Weckert for their support and their interest during the compilation of this work.

References

- [1] M. Altarelli, et al. (Eds.) XFEL, The European X-ray Free-Electron Laser, Technical Design Report, DESY 2006-097, Hamburg (2006).
- [2] Y. Li et al., 2008, Study of Controllable Polarization SASE FEL by a Crossed-planar Undulator, Proc. EPAC08, Genoa, Italy.

- [3] B. Faatz et al., 2008, Study of Controllable Polarization of a SASE FEL Using a Crossed-planar Undulator, Proc. FEL 2008, Gyeongju, Korea.
- [4] Y. Li, B. Faatz and J. Pflueger, 2010, Polarization properties of crossed planar undulators, Nucl. Instrum. Meth. A 613 (2010), 163.
- [5] Y. Li et al. 2010, Microbunch preserving bending system for a helical radiator at the European XFEL, Phys. Rev. ST Accel. Beams 13 (2010), 080705.
- [6] E.A. Schneidmiller, M.V. Yurkov, 2010, An Option of Frequency Doubler at the European XFEL for Generation of Circularly Polarized Radiation in the Wavelength Range Down to 1 - 2.5 nm, FEL 2010, Malm, Sweden.
- [7] G. Geloni, V. Kocharyan and E. Saldin, Microbunch preserving in-line system for an APPLE II helical radiator at the LCLS baseline, DESY 11-083 (2011)
- [8] J. Bahrtdt et al., EPAC Conference Proceedings 2008 p 2219, "APPLE undulator for PETRA III" (2008)
- [9] S Reiche et al., Nucl. Instr. and Meth. A 429, 243 (1999).
- [10] Igor Zagorodnov, Private communication.
- [11] G. Geloni, V. Kocharyan and E. Saldin, "The effects of betatron motion on the preservation of FEL microbunching", DESY 11-081 (2011).